

# The Formation and Fragmentation of Primordial Molecular Clouds

Tom Abel<sup>1</sup>, Greg L. Bryan<sup>2,3</sup> and Michael L. Norman<sup>4,5</sup>

<sup>1</sup>*Harvard Smithsonian Center for Astrophysics, MA, US-02138 Cambridge*

<sup>2</sup>*Massachusetts Institute of Technology, MA, US-02139 Cambridge*

<sup>3</sup>*Hubble Fellow*

<sup>4</sup>*LCA, NCSA, University of Illinois, US-61801 Urbana/Champaign*

<sup>5</sup>*Astronomy Department, University of Illinois, Urbana/Champaign*

## Abstract

Many questions in physical cosmology regarding the thermal history of the intergalactic medium, chemical enrichment, reionization, etc. are thought to be intimately related to the nature and evolution of pregalactic structure. In particular the efficiency of primordial star formation and the primordial IMF are of special interest. We present results from high resolution three-dimensional adaptive mesh refinement simulations that follow the collapse of primordial molecular clouds and their subsequent fragmentation within a cosmologically representative volume. Comoving scales from 128 kpc down to 1 pc are followed accurately. Dark matter dynamics, hydrodynamics and all relevant chemical and radiative processes (cooling) are followed self-consistently for a cluster normalized CDM structure formation model. Primordial molecular clouds with  $\sim 10^5$  solar masses are assembled by mergers of multiple objects that have formed hydrogen molecules in the gas phase with a fractional abundance of  $\lesssim 10^{-4}$ . As the subclumps merge cooling lowers the temperature to  $\sim 200$  K in a “cold pocket” at the center of the halo. Within this cold pocket, a quasi-hydrostatically contracting core with mass  $\sim 200 M_\odot$  and number densities  $\gtrsim 10^5 \text{ cm}^{-3}$  is found. We find that less than 1% of the primordial gas in such small scale structures cools and collapses to sufficiently high densities to be available for primordial star formation. Furthermore, it is worthwhile to note that this study achieved the highest dynamic range covered by structured adaptive mesh techniques in cosmological hydrodynamics to date.

## 1. Introduction

Saslaw and Zipoy (1967) realized the importance of gas phase  $\text{H}_2$  molecule formation in primordial gas for the formation of proto-galactic objects. Employing this mechanism in Jeans unstable clouds, Peebles and Dicke (1968) formulated their model for the formation of primordial globular clusters. Further pioneering studies in this subject were carried out by Takeda *et al.* (1969), Matsuda *et al.* (1969), and Hirasawa *et al.* (1969) who followed in detail the gas kinetics in collapsing objects and studied the possible formation of very massive objects (VMO’s). In the 1980’s the possible cosmological consequences of population III

star formation were assessed (Rees and Kashlinsky 1983; Carr *et al.* 1984; Couchman and Rees 1986). In particular Couchman and Rees (1986) discussed first structure formation within the standard cold dark matter model. Their main conclusions were that the first objects might reheat and reionize the universe, raise the Jeans mass and thereby influence subsequent structure formation.

Early studies focused on the chemical evolution and cooling of primordial clouds by solving a chemical reaction network within highly idealized collapse models (cf. Hirasawa 1969; Hutchins 1976; Palla *et al.* 1983; MacLow and Shull 1986; Puy *et al.* 1996; Tegmark *et al.* 1997). Some hydrodynamic aspects of the problem were stud-

ied in spherical symmetry by Bodenheimer (1986) and Haiman, Thoul and Loeb (1996). Recently multi-dimensional studies of first structure formation have become computationally feasible (Abel 1995; Anninos & Norman 1996; Zhang *et al.* 1997; Gnedin & Ostriker 1997; Abel *et al.* 1998a,1998b; Bromm *et al.* 1999). These investigations have provided new insights into the inherently multidimensional, nonlinear, nonequilibrium physics which determine the collapse and fragmentation of gravitationally and thermally unstable primordial gas clouds.

In Abel, Anninos, Norman & Zhang 1998a (hereafter AANZ) we presented the first self-consistent 3D cosmological hydrodynamical simulations of first structure formation in a standard cold dark matter-dominated (SCDM) universe. These simulations included a careful treatment of the formation and destruction of  $H_2$  —the dominant coolant in low mass halos ( $M_{tot} = 10^5 - 10^8 M_\odot$ ) which collapse at high redshifts ( $z \sim 30 - 50$ ). Among the principal findings of that study were: (1) appreciable cooling only occurs in the cores of the high density spherical knots located at the intersection of filaments; (2) good agreement was found with semi-analytic predictions (Abel 1995; Tegmark *et al.* 1997) of the minimum halo mass able to cool and collapse to higher densities; (3) only a small fraction ( $< 10\%$ ) of the bound baryons are able to cool promptly, implying that primordial Pop III star clusters may have very low mass. Due to the limited spatial resolution of the those simulations ( $\sim 1$  kpc *comoving*), we were unable to study the collapse to stellar densities and address the nature of the first objects formed.

In this paper we present new, higher- resolution results using the powerful numerical technique of adaptive mesh refinement (AMR, Bryan & Norman 1997; Norman & Bryan 1999) which has shed some light on how the cooling gas fragments. With an effective dynamic range of 262, 144 the numerical simulations presented here are the highest resolution simulations in cosmological hydrodynamics to date. Although we are not yet able to form individual protostars, we are able to resolve the collapsing protostellar cloud cores which must inevitably form them. We find the cores have typical masses  $\sim 200 M_\odot$ , sizes  $\sim 0.3$  pc, and number densities  $n \geq 10^5 \text{ cm}^{-3}$ —similar to dense molec-

ular cloud cores in the Milky Way with one vital difference: the molecular hydrogen fraction is  $\sim 5 \times 10^{-4}$ , meaning the cores evolves very differently from Galactic cores.

The plan of this paper is as follows. The simulations are briefly described in Sec. 2. Results are presented in Sec. 3. The properties and fate of the primordial protostellar cloud are discussed in Sec. 4. Conclusions follow in Sec. 5. Results of a broader survey of simulations will be reported in Abel, Bryan & Norman (1999).

## 2. Simulations

The three dimensional adaptive mesh refinement calculations presented here use for the hydrodynamic portion an algorithm very similar to the one described by Berger and Collela (1989). The code utilizes an adaptive hierarchy of grid patches at various levels of resolution. Each rectangular grid patch covers some region of space in its parent grid needing higher resolution, and may itself become the parent grid to an even higher resolution child grid. Our general implementation of AMR places no restriction on the number of grids at a given level of refinement, or the number of levels of refinement. However, we do restrict the refinement factor — the ratio of parent to child mesh spacing — to be an integer (chosen to be 2 in this work). The dark matter is followed with methods similar to the ones presented by Couchman (1991). Furthermore, the algorithm of Anninos *et al.* (1997) is used to solve the time-dependent chemistry and cooling equations for primordial gas given in Abel *et al.* (1997). More detailed descriptions of the code are given in Bryan & Norman (1997, 1999), and Norman & Bryan (1999).

The simulations are initialized at redshift 100 with density perturbations of a SCDM model with  $\Omega_B = 0.06$ ,  $h = 0.5$ , and  $\sigma_8 = 0.7$ . The abundances of the 9 chemical species ( $H$ ,  $H^+$ ,  $H^-$ ,  $He$ ,  $He^+$ ,  $He^{++}$ ,  $H_2$ ,  $H_2^+$ ,  $e^-$ ) and the temperature are initialized as discussed in Anninos and Norman (1996). After a collapsing high- $\sigma$  peaks has been identified in a low resolution run, the simulation is reinitialized with multiple refinement levels covering the Lagrangian volume of the collapsing structure. The mass resolution in the initial conditions within this region are  $0.53(8.96) M_\odot$  in the gas (dark matter). The refinement criteria en-

sure that: (1) the local Jeans length is resolved by at least 4 grid zones, and (2) that no cell contains more than 4 times the initial mass element ( $0.53 M_{\odot}$ ). We limit the refinement to 12 levels within a  $64^3$  top grid which translates to a maximum dynamic range of  $64 \times 2^{12} = 262,144$ .

### 3. Results

We find that primordial molecular clouds are only formed at the intersection of filaments, in agreement with the results of AANZ. The evolution of these primordial molecular clouds is marked by frequent mergers yielding highly complex velocity and density fields within the “virial” radius. In the following three sections, we first describe the evolution of these objects and then their morphology and structure.

#### 3.1. Formation of the First Objects

To illustrate the physical mechanisms at work during the formation of the first cosmological object in our simulation, we show the evolution of various quantities in Figure 1. The top panel of this plot shows the virial mass of the largest object in the simulation volume. We divide the evolution up into four intervals. In the first, before a redshift of about 35, the Jeans mass in the baryonic component is larger than the mass of any non-linear perturbation. Therefore, the only collapsed objects are dark-matter dominated, and the baryonic field is quite smooth. (We remind the reader that a change in the adopted cosmological model would modify the timing, but not the nature, of the collapse.)

In the second epoch,  $23 < z < 35$ , as the non-linear mass increases, the first baryonic objects collapse. However, these cannot efficiently cool and the primordial entropy of the gas prevents dense cores from forming. This is shown in the second frame of figure 1 by a large gap between the central baryonic and dark matter densities (note that while the dark matter density is limited by resolution, the baryonic is not, so the true difference is even larger). As mergers continue and the mass of the largest clump increases, its temperature also grows, as shown in the third panel of this figure. The  $H_2$  fraction also increases (bottom panel).

By  $z \sim 23$ , enough  $H_2$  has formed (a few

$\times 10^{-4}$ ), and the temperature has grown sufficiently high that cooling begins to be important. During this third phase, the central temperature decreases and the gas density increases. However, the collapse is somewhat protracted because around this point in the evolution, the central density reaches  $n \sim 10^4 \text{ cm}^{-2}$ , and the excited states of  $H_2$  are in LTE. This results in a cooling time which is nearly independent of density rather than in the low-density limit where  $t_{cool} \sim \rho^{-1}$  (e.g. Lepp & Shull 1983).

Finally, at  $z \sim 19$ , a very small dense core forms and reaches the highest resolution that we allowed the code to produce. It is important to note that at this point, the maximum gas density in the simulations exceeds  $10^8 \text{ cm}^{-3}$ , and at these densities, 3-body formation of molecular hydrogen will become dominant (see Palla *et al.* 1983). Also, the assumption of optical thin cooling begins to break down and radiative transfer effects become important. Therefore, only simulation results at and above this redshift will be discussed. It is worthwhile to note that the simulations presented here are physics rather than resolution limited.

#### 3.2. Morphology

The increase in dynamic range by  $\sim 1000$  in the simulations presented here as compared to AANZ allow us to investigate the details of the fragmentation process in detail. Visualizations of the gas density and temperature on two different scales at  $z = 19.1$  are shown in the color plate 3. In the upper left panel the velocity field is shown superimposed on the density. The  $5 \times 10^5 M_{\odot}$  structure forms at the intersection of two filaments with overdensities of  $\sim 10$ . Most of the mass accretion occurs along these filaments. The complexity of the velocity field is evident; the accretion shock is highly aspherical and of varying strength. Within the virial radius ( $r = 106 \text{ pc}$ ), there are a number of other cooling regions. The right-hand panels zooms in on the collapsing fragment. (note that the smallest resolution element ( $0.02 \text{ pc}$ ) in the simulations is still 1600 times smaller than the slice shown in the right panels). The small fragment in the center of this image has a typical overdensity of  $\gtrsim 10^6$  and a mass of  $\sim 200 M_{\odot}$ .

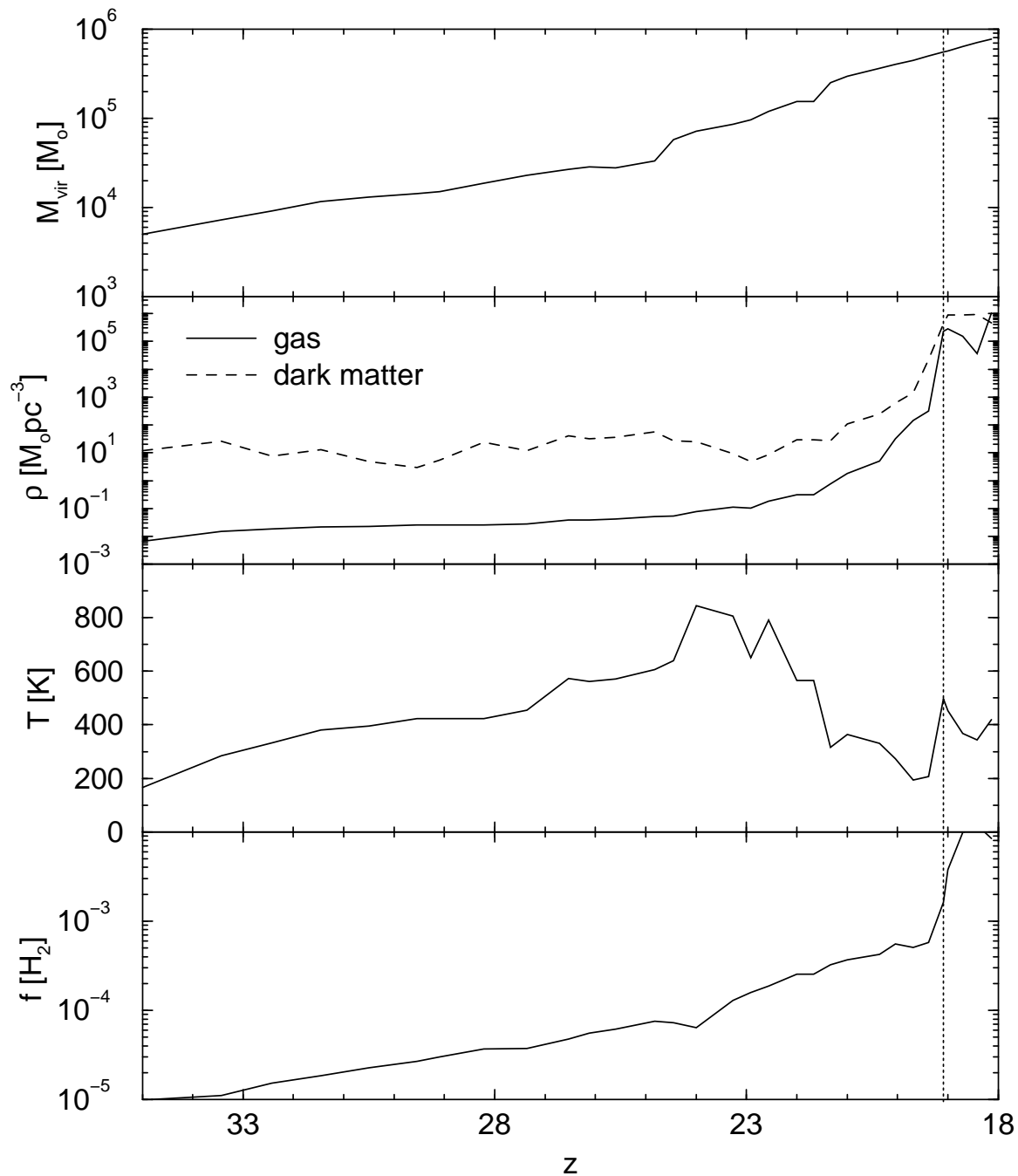


Fig. 1.— The top panel shows the evolution of the virial mass of the most massive clump as a function of redshift. The remaining panels show the density (both dark and baryonic), the temperature, and the molecular hydrogen mass fraction at the central point of that clump. The central point is defined as the point with the highest baryon density. Clearly the finite gas pressure prevents baryons from clumping as much as the dark matter at redshifts  $\gtrsim 23$ . The vertical line at  $z = 19.1$  indicates where our numerical model breaks down.

### 3.3. Profiles

Despite the complex structure of the primordial molecular clouds much of their structure can be understood from spherical profiles of the physical quantities, particularly for the dense central core which is nearly spherical. Figure 3.3 shows mass-weighted, spherical averages of various quantities around the densest cell found in the simulation at redshift 19.1. Panel a) plots the baryon number density, enclosed baryon mass, and local Bonnor-Ebert mass<sup>1</sup>  $\approx 27 M_{\odot} T_K^{1.5} / \sqrt{n}$  versus radius. Panel b) plots the abundances of H<sub>2</sub> and free electrons. Panel c) compares three timescales defined locally: the H<sub>2</sub> cooling time  $t_{H_2}$ , the freefall time  $t_{ff} = [3\pi/(32G\rho)]^{1/2}$ , and the sound crossing time  $t_{cross} = r/c_s = 7.6 \times 10^6 r_{pc} / \sqrt{T_K}$  yrs. In panel d) we identify two distinct regions—labeled I and II—as defined by the temperature profile. Region I ranges from outside the virial radius to  $r_{T_{min}} \sim 5$  pc, the radius at which the infalling material has cooled down to  $T_{min} \sim 200$  K—near the minimum temperature allowed by H<sub>2</sub> cooling. Within region I, the temperature profile reflects, in order of decreasing radius, cosmic infall, shock virialization, adiabatic heating in a settling zone, and an H<sub>2</sub> cooling flow. In region II, the temperature slowly rises from  $T_{min}$  to  $\sim 400$  K due to adiabatic heating.

For most of region I the H<sub>2</sub> cooling time  $t_{H_2}$  is comparable to the free-fall time, as is illustrated in panel c) of Figure 3.3. The H<sub>2</sub> number fraction rises from  $7 \times 10^{-6}$  to  $2 \times 10^{-4}$  as the free electron fraction drops from  $2 \times 10^{-4}$  to  $2 \times 10^{-5}$ . At  $r_{T_{min}}$ , the sound crossing time becomes substantially shorter than the cooling time. This suggests that region II is contracting quasi-hydrostatically on the cooling time scale, which approaches its constant high-density value at small radii. This constant cooling time of  $\sim 10^5$  years sets the time scale of the evolution of the fragment until it can turn fully molecular via three body associations. Inside  $r \sim 0.3$  pc, the enclosed baryonic mass of  $\sim 200 M_{\odot}$  exceeds the local Bonnor-Ebert mass, implying this material is gravitationally unstable. However, due to the inefficient cooling, its collapse is subsonic (panel e). The radius where  $M > M_{BE}$

<sup>1</sup>Bonnor-Ebert mass is the analog of the Jeans Mass but assuming an isothermal ( $\rho \propto r^{-2}$ ) instead of a uniform density distribution.

defines our protostellar cloud core.

### 4. Discussion

Many interesting features of the collapsing and fragmenting “primordial molecular cloud” are identified. Most notable is the formation of an initially quasi-hydrostatically contracting core of  $\sim 200 M_{\odot}$  which becomes gravitationally unstable. We argue that this is a characteristic mass scale for core formation mediated by H<sub>2</sub> cooling. Substituting into the formula for the Bonnor-Ebert mass  $T_{min}$  and  $n_{LTE}$  we get  $240 M_{\odot}$ .

What will be the fate of the collapsing core? Within the core the number densities increase from  $10^5$  to  $10^8$  cm<sup>-3</sup>. For densities  $\gtrsim 10^8$  cm<sup>-3</sup>, however, three-body formation of H<sub>2</sub> will become the dominant formation mechanism, transforming all hydrogen into its molecular form (Palla *et al.* 1983). Our chemical reaction network does not include this reaction and the solution cannot be correct at  $r \lesssim 0.1$  pc. The most interesting effect of the three-body reaction is that it will increase the cooling rate by a factor  $\sim 10^3$ , leading to a further dramatic density enhancement within the core. This will decrease the dynamical timescales to  $\ll 100$  years, effectively decoupling the evolution of the fragment from the evolution of its host primordial molecular cloud. Therefore, it is a firm conclusion that only the gas within these cores can participate in population III star formation.

Omukai & Nishi (1998) have simulated the evolution of a collapsing, spherically symmetric primordial cloud to stellar density including all relevant physical processes. Coincidentally, their initial conditions are very close to our final state. Based on their results, we can say that if the cloud does not break up, a massive star will be formed. Adding a small amount of angular momentum to the core does not change this conclusion (Bate 1998). A third possibility is that the cloud breaks up into low mass stars via thermal instability in the quasi-hydrostatic phase. Silk (1983) has argued that, due to the enhanced cooling from the 3-body produced H<sub>2</sub>, fragmentation of this core might continue until individual fragments are opacity limited (i.e. they become opaque to their cooling radiation). Exploring which of these scenarios is correct will have to await yet higher res-

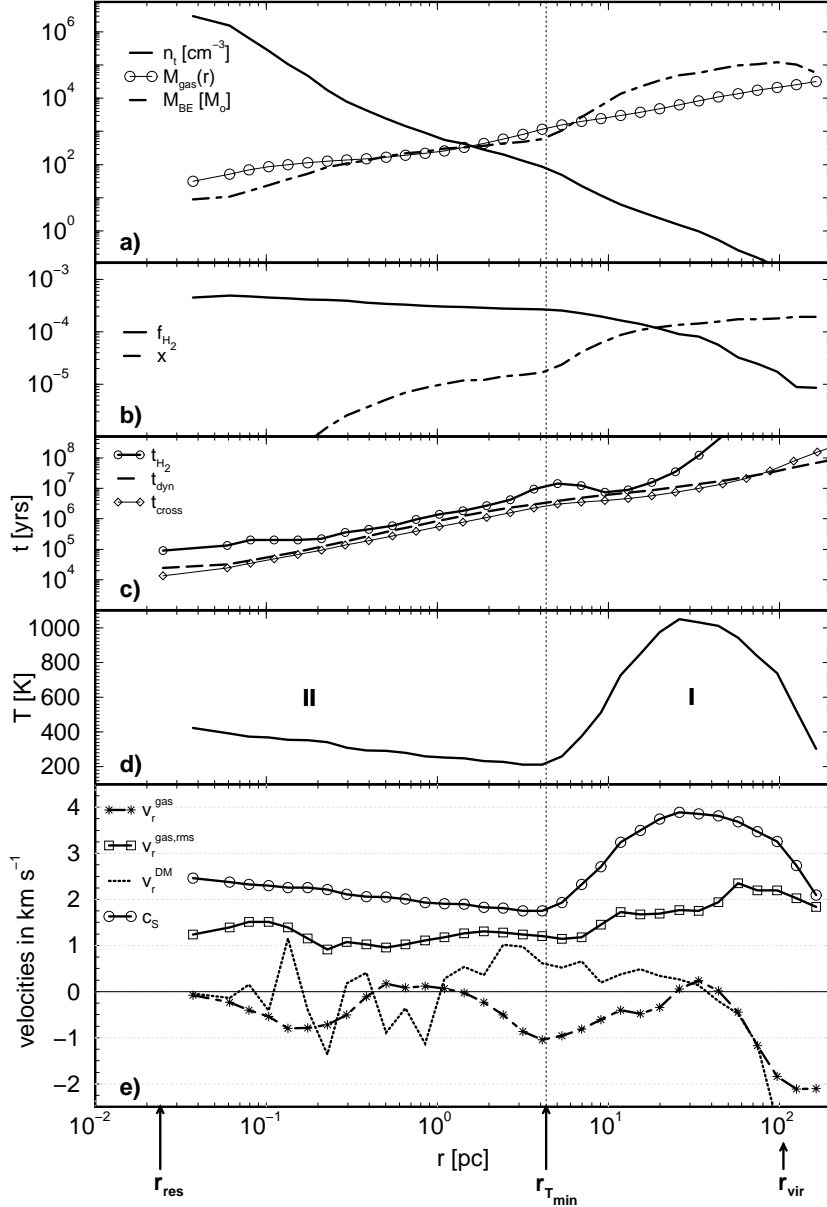


Fig. 2.— Spherically averaged mass weighted profiles around the baryon density peak shortly before a well defined fragment forms ( $z=19.1$ ). Panel a) shows the baryonic number density, enclosed gas mass in solar mass, and the local Bonnor–Ebert mass ( $\approx 27 M_{\odot} T_K^{1.5}/\sqrt{n}$ ). Panel b) plots the molecular hydrogen number fraction  $f_{H_2}$  and the free electron number fraction  $x$ . The  $H_2$  cooling time  $t_{H_2}$ , the time it takes a sound wave to travel to the center,  $t_{cross}$ , and the free-fall time  $t_{ff} = [3\pi/(32G\rho)]^{1/2}$  are given in panel c). Panel d) gives the temperature in Kelvin as a function of radius. The bottom panel gives the local sound speed,  $c_s$  (solid line with circles), the rms radial velocities of the dark matter (dashed line) and the gas (dashed line with asterisks) as well as the rms gas velocity (solid line with square symbols). The vertical dotted line indicates the radius at which the gas has reached its minimum temperature allowed by  $H_2$  cooling ( $\sim 5pc$ ). The virial radius of the  $5.6 \times 10^6 M_{\odot}$  halo is 106 pc. The cell size on the finest grid corresponds to 0.024 pc. Note that the simulation box size corresponds to 6.4 proper kpc.

olution simulations including the effects of radiative transfer. It will also be interesting to examine the possible effects of molecular HD which, although much less abundant, is a much more efficient coolant at low temperatures.

How many cores are formed in our halo? Because our timestep contracts rapidly once the first core forms, we are not yet able to answer this question definitively. An earlier, less well resolved simulation yielded 5 – 6 cores by  $z = 16.5$ , suggesting that multiple cores do form. We speculate that the total number of cores to eventually form will be proportional to the total amount of cooled gas. However, the first star in a given halo will most likely always be formed close to its center where the dynamical timescale is shortest. The cooling timescale at  $r_{T_{min}}$  in Figure 2. of  $\gtrsim 10^6$  years should roughly correspond to the typical formation time of fragments. During this time the product of the first collapsed fragment might already be an important source of feedback. Hence, even for the question of the efficiency of fragmentation it seems that feedback physics have to be included.

Let us assume the first  $\sim 200 M_{\odot}$  cores fragment to form stars with 100% efficiency. If the ratio of produced UV photons per solar mass is the same as in present day star clusters than about  $6 \times 10^{63}$  UV photons would be liberated during the average life time of massive star ( $\sim 5 \times 10^7$  years). This is about hundred times more than the  $\sim 4 \times 10^{61}$  hydrogen atoms within the virial radius. However, the average recombination time  $(nk_{rec})^{-1} \sim 5 \times 10^5$  years within the virial radius is a factor 100 less than the average lifetime of a massive star. Hence, very small or zero UV escape fractions for these objects are plausible. However, the first supernovae and winds from massive stars will substantially change the subsequent hydrodynamic and chemical evolution as well as the star formation history of these objects. A more detailed understanding of the role of such local feedback will have to await yet more detailed simulations that include the poorly understood physics of stellar feedback mechanisms.

Since the collapsing core evolves on much faster timescales than the rest of the halo it seems plausible that the first star (or star cluster) will have a mass of less or the order of the core mass. It seems also quite clear that the radiative feedback from this star (these stars) will eventually halt fur-

ther accretion. As a consequence this might suggest that the formation of very massive objects or supermassive black holes is unlikely. This later speculation will be tested by yet higher resolution simulations we are currently working on.

Recently Bromm, Coppi, and Larson (1999) have studied the fragmentation of the first objects in the universe. The results of their simulations using a smooth particle hydrodynamics technique with isolated boundary conditions disagree with the results presented here. Their objects collapse to a disk which then fragments quickly to form many fragments throughout the rotationally supported disk. The efficiently fragmenting disk in those simulations originates from the assumed idealized initial conditions. These authors simulated top-hat spheres that initially rotate as solid bodies on which smaller density fluctuations were imposed. Naturally they find a disk. Also it is clear that for a top-hat if the disk breaks up it will do so everywhere almost simultaneously. Our results with realistic initial conditions do not lead to a disk and form the first fragment close to the center of the halo.

## 5. Conclusions

We have reported first results from an ongoing project that studies the physics of fragmentation and primordial star formation in a cosmological context. The results clearly illustrate the advantages and power of structured adaptive mesh refinement cosmological hydrodynamic methods to cover a wide range of mass, length and timescales. All findings of AANZ are confirmed in this study. Among other things, these are that 1) a significant number fraction of hydrogen molecules is only formed in virialized halos at the intersection of filaments, and 2) only a few percent of the halo gas has cooled to  $T \ll T_{vir}$ .

The improvement of a factor  $\sim 1000$  in resolution over AANZ has given new insights into the details of the fragmentation process and constraints on the possible nature of the first structures: 1) Only  $\lesssim 1\%$  of the baryons within a virialized object can participate in population III star formation. 2) The formation of super massive black holes or very massive objects in small halos seem very unlikely. 3) Fragmentation via Bonnor–Ebert instability yields a  $\sim 200 M_{\odot}$  core within

one virialized object. 4) If the gas were able to fragment further through 3-body  $H_2$  association and/or opacity limited fragmentation, only a small fraction of all baryons in the universe will be converted into small mass objects. 5) The escape fraction of UV photons above the Lyman limit should initially be small due to the high column densities of HI ( $N_{HI} \sim 10^{23} \text{ cm}^{-2}$ ) of the parent primordial molecular cloud. 6) The first star in the universe is most likely born close to the center of its parent halo of  $\gtrsim 10^5 M_\odot$ .

This work is supported in part by NSF grant AST-9803137 under the auspices of the Grand Challenge Cosmology Consortium (GC<sup>3</sup>). NASA also supported this work through Hubble Fellowship grant HF-0110401-98A from the Space Telescope Science Institute, which is operated by the Association of Universities for Research in Astronomy, Inc under NASA contract NAS5-26555. Tom Abel acknowledges support from NASA grant NAG5-3923 and useful discussions with Karsten Jedamzik, Martin Rees, Zoltan Haiman, and Simon White.

## REFERENCES

- Abel, T. 1995, Thesis, University of Regensburg, Germany
- Abel, T., Anninos, P., Zhang, Y., Norman, M.L. 1997, *NewA*, 2, 181
- Abel, T., Anninos, P., Norman, M.L., Zhang, Y. 1998a (AANZ), *ApJ*, 508, 518.
- Abel, T., Bryan, G.L., Norman, M.L. 2000, in preparation.
- Abel, T., Stebbins, A., Anninos, P., Norman, M.L. 1998b, *ApJ*, 508, 530.
- Anninos, P., Norman, M.L. 1996, *ApJ*, 460, 556
- Anninos, P., Zhang, Y., Abel, T., Norman, M.L. 1997, *NewA*, 2, 209
- Bate, M. 1998. *ApJL*, 508, 95
- Berger, M.J., Collela, P. 1989, *J. Comp. Phys.*, 82, 64
- Bertoldi, F., Draine, B. T. 1996, *ApJ*, 458, 222
- Bodenheimer, P.H. 1986, *Final Technical Report, California Univ., Santa Cruz.*
- Bromm, V., Coppi, P., Larson, R.B. 1999, *ApJL*, 527, L5
- Bryan, G.L., Norman, M.L. 1997, in *Computational Astrophysics*, eds. D.A. Clarke and M. Fall, ASP Conference #123
- Bryan, G.L., Norman, M.L. 1999, in *Workshop on Structured Adaptive Mesh Refinement Grid Methods*, IMA Volumes in Mathematics No. 117, ed. N. Chrisochoides, p. 165
- Carr, B.J., Bond, J.R., Arnett, W.D. 1984, *ApJ*, 277, 445
- Couchman, H. 1991, *ApJL*, 368, L23
- Gnedin, N.Y., Ostriker, J.P. 1997, *ApJ*, 486, 581
- Haiman, Z., Thoul, A.A., Loeb, A. 1996, *ApJ*, 464, 523
- Hirasawa, T. 1969, *Progr. Theoret. Phys.*, 42, 523
- Hoyle, F. 1953, *ApJ*, 118, 513
- Hutchins, J.B. 1976, *ApJ*, 205, 103
- Kashlinsky, A., Rees, M.J. 1983, *MNRAS*, 205, 955
- Lepp, S., & Shull, J.M. 1983, *ApJ*, 270, 578
- Mac Low, M.-M. & Shull, J.M. 1986, *ApJ*, 302, 585
- Matsuda, T., Sato, H., Takeda, H. 1969, *Progr. Theoret. Phys.*, 41, 840
- Norman, M.L., Bryan, G.L. 1998, in *Numerical Astrophysics 1998*, eds. S. Miyama & K. Tomisaka
- Omukai, K. & Nishi, R. 1998. *ApJ*, 508, 1410.
- Palla, F., Salpeter, E.E., Stahler, S.W. 1983, *ApJ*, 271, 632
- Padmanabhan, T. 1993, *Structure formation in the universe*, Cambridge University Press
- Peebles, P.J.E., Dicke, R.H. 1968, *ApJ*, 154, 891
- Puy, D., Signore, M. 1996, *A&A*, 305, 371
- Saslaw, W.C., & Zipoy, D. 1967, *Nature*, 216, 976
- Silk, J. 1983, *MNRAS*, 205, 705
- Takeda, H., Sato, H., Matsuda, T. 1969, *Progr. Theoret. Phys.*, 41, 840
- Tegmark, M., Silk, J., Rees, M.J., Blanchard, A., Abel, T., Palla, F. 1997, *ApJ*, 474, 1
- Zhang, Y., Norman, M.L., Anninos, P., & Abel, T. 1997, in S.S. Holt and L.G. Mundy, eds., *Star formation, near and far*, AIP Press, New York, 329

---

This 2-column preprint was prepared with the AAS L<sup>A</sup>T<sub>E</sub>X macros v5.0.

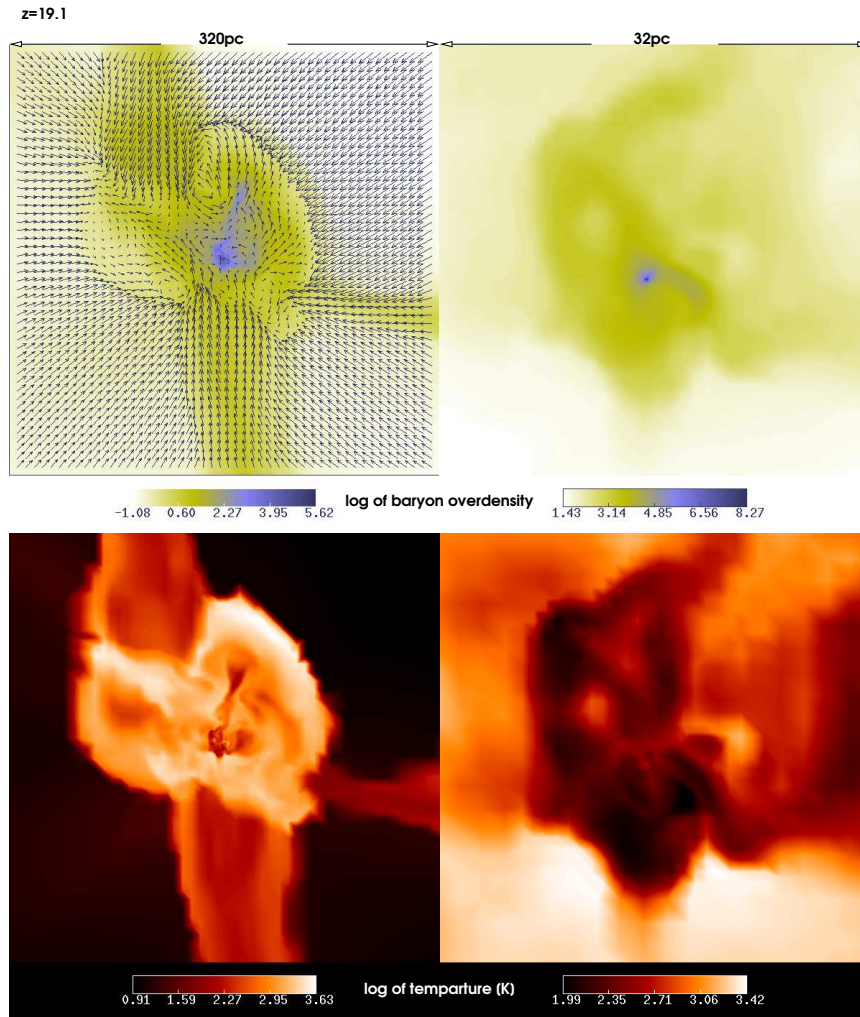


Fig. 3.— Gas density and temperature in the first cosmological objects expected to form in hierarchical structure formation scenarios. The upper panels show the log of the baryonic overdensity in a slice through the point of highest gas density at a scale of 320 pc (left) and 32 pc (right). The lower panels give the corresponding plots of the log of the gas temperature. Additionally the velocity field is also visualized in the upper left panel. Note that the computational volume simulated is  $20^3$  times larger than the left panels.